

Effect of ^4He on the surface scattering of ^3He

S. M. Tholen* and J. M. Parpia

Laboratory of Atomic and Solid State Physics, Cornell University, Ithaca, New York 14853-2501

(Received 20 May 1992; revised manuscript received 6 August 1992)

We describe and compare the results of two investigations in which the boundary condition for ^3He was altered by the addition of ^4He , which is preferentially confined to the surfaces by virtue of its smaller zero-point motion. In the first experiment, carried out in normal ^3He , we observed an increase of specularly in the slip between ^3He and the polished silicon substrate at a coverage consistent with the onset of superfluidity in the surface ^4He layer. The second experiment was performed on superfluid ^3He confined within the pores of sintered silver. By coating the surfaces with ^4He , we observed a partial restoration of the superfluid fraction and transition temperature, which had been reduced below bulk by finite-size effects. This effect is due to a change from diffuse to specular boundary scattering. We found that the specularly induced by the ^4He was destroyed upon the application of a pressure sufficient to solidify the surface ^4He , confirming the role of surface superfluid ^4He on specular scattering.

I. INTRODUCTION

We document the results of two torsional oscillator experiments designed to investigate the nature of ^3He scattering at a solid boundary. The first¹ was performed on normal ^3He , where the surface scattering determines the amount of slip or velocity difference between the fluid and the substrate. These measurements were carried out first for pure ^3He ; subsequently, various amounts of ^4He were introduced before admitting the ^3He . The ^4He is preferentially coated onto the surfaces since its zero-point motion is smaller than that of ^3He . We were able to map out in detail the changes in slip that occur upon the addition of ^4He . The results suggested that the superfluidity of the ^4He layer might be responsible for the increased specularly observed.

The second experiment² was performed on superfluid ^3He confined to a restricted geometry. The superfluid density near the walls is suppressed in such a system if the scattering is diffuse. ^4He was added to the surfaces after completing measurements on pure ^3He , and we verified that the increased specularly observed for the normal fluid also occurred for superfluid ^3He . By varying the pressure in this cell we found that the specularly induced by the ^4He was completely destroyed when the ^4He was solidified.

II. NORMAL ^3He EXPERIMENT

A. Motivation

The earliest experiments which investigated the boundary condition for fluid flow of ^3He suggested that the surface scattering was diffuse for a variety of substrates.^{3,4} Classically one would expect that a light, fast-moving particle striking a massive wall would be an almost completely elastic collision. In the absence of multiple collisions caused by an extremely rough or irregular surface, the scattering would be specular (with the component of momentum parallel to the surface unchanged by the col-

lision). The roughness size relevant to scattering is not clear for ^3He . One might describe the size of ^3He using the mean thermal wavelength, $\Lambda = h / \sqrt{2\pi m^* k_B T}$, which ranges from about 60 Å at 10 mK to about 180 Å at 1 mK. To make a surface smooth on this length scale is quite feasible and could induce specular scattering. Alternatively, the fermionic nature of ^3He might suggest that the appropriate size is the inverse Fermi wave number, k_F^{-1} . If true, then the ^3He size would be around 1.2 Å, so all surfaces would be rough compared to this length scale and would be expected to scatter ^3He diffusely.

Previous experiments designed specifically to measure slip^{3,5} found that the slip was substantially smaller than the theoretical prediction for completely diffuse scattering. Including any specular scattering would further increase the discrepancy. This was an indication that surface effects were not accurately described by slip theory.

Other experiments^{6,7} performed on mixtures of ^3He and ^4He also showed discrepancies with slip theory. Although these measurements were not sensitive to very small slip, they were able to see slip increase substantially when the equivalent of several surface monolayers of ^4He were present. However, while the addition of ^4He seemed to increase the specularly of the surfaces, the measured quantities did not have the temperature dependence predicted by slip theory. Due to their geometries, these experiments were unable to probe the onset and abruptness of the transition from diffuse to specular scattering. They were therefore unable to see if the disagreement with slip theory coincided with the onset of specularly. It was also found in a separate experiment⁸ on superfluid ^3He that adding a few monolayers of ^4He to the surfaces changed the scattering from diffuse to nearly 100% specular. It was proposed that the effect of the ^4He was to smooth atomic-sized corrugations on the surfaces and thus induce specularly.

The initial intent of our experiment on normal ^3He was twofold. First, we wished to determine whether or not surfaces that were smooth compared to the mean thermal wavelength of ^3He would scatter specularly. Second, we

wanted to investigate in detail the effects of surface ^4He . We chose silicon for our substrate because we could polish it to $\approx 20 \text{ \AA}$ roughness (on a horizontal scale of about 1000 \AA). At the coldest temperatures, this roughness is well below Λ . We also chose a simple geometry with a large ratio of surface area to volume to enhance the slip term.

B. Background

In the normal fluid, the surface scattering of ^3He atoms is manifested in the slip, or velocity difference between the fluid and the wall. Conventional hydrodynamics assumes that the relative velocity of a fluid goes to zero at any boundary. In actuality, however, the slip is always nonzero and dependent on the nature of the fluid and its scattering. For completely specular scattering, there is no momentum transfer parallel to the surface and the slip is infinite. For completely diffuse scattering, the momentum transfer is maximized and the slip minimized.

The slip of a fluid affects its hydrodynamic properties primarily through its viscosity. The viscosity of normal ^3He in the Landau-Fermi liquid regime is given by⁹

$$\eta = \frac{1}{5} n p_F \lambda, \quad (1)$$

where n is the number density of the ^3He , p_F is the Fermi momentum, and λ is the mean free path. At a given pressure, both n and p_F are independent of temperature. At low temperatures ($T \ll T_F$), the mean free path varies as T^{-2} . Many experiments have verified for bulk ^3He that $\eta = A/T^2$ for temperatures below about 15–20 mK. The values found^{3,5–7} for A cluster around roughly $2.35 \text{ mK}^2 \text{ P}$ for 0 bar.¹⁰

In bulk fluid near an oscillating plane, the relative fluid velocity decays to zero (assuming no slip) near the boundary over a characteristic length scale δ , the viscous penetration depth. This length is determined by the viscosity of the fluid and is given by

$$\delta = \sqrt{2\eta/\rho\omega}. \quad (2)$$

Here, ρ is the density of the fluid and ω is the frequency of oscillation. The viscous penetration depth is inversely proportional to temperature due to the T^{-2} dependence of η . For ^3He is 0 bar, at 1600 Hz (the resonant frequency of our oscillator), we expect $\delta \sim 755/T \text{ \mu m}$ (with T in mK).

The slip approximation introduces first-order corrections to classical hydrodynamics due to slip. The relative velocity of the fluid is finite at a boundary but can be extrapolated to zero at a distance ζ behind the wall.¹¹ The slip length ζ is proportional to the mean free path λ . When slip is included in the hydrodynamic description of fluid flow in a parallel plate geometry of height d , the equations are unchanged (in the limit that $\zeta, \lambda < d$) if one simply replaces the bulk viscosity with an effective viscosity¹¹ given by

$$\frac{1}{\eta_{\text{eff}}} = \frac{1}{\eta} \left[1 + \frac{6\zeta}{d} \right]. \quad (3)$$

This can be rewritten using Eq. (1) as

$$\frac{1}{\eta_{\text{eff}}} = \frac{1}{\eta} + \frac{30}{n p_F d} \left[\frac{\zeta}{\lambda} \right] = \frac{1}{\eta} + \text{const}. \quad (4)$$

Since slip length is proportional to mean free path, the second term in Eq. (4) is independent of temperature. Its magnitude is determined by the amount of slip, which in turn depends on the type of scattering the ^3He experiences at the surfaces. For a flat surface, this term is always positive (although the special case of surfaces with large mesoscopic curvature can allow for zero or even negative slip and will be discussed later), but is minimized for completely diffuse scattering. For partially specular scattering, we can assume that some fraction, s , of the incoming ^3He atoms are specularly reflected from the surface and the remaining $1-s$ are scattered diffusely. Slip theory¹² then finds for ^3He that the ratio of slip length to mean free path is

$$\frac{\zeta}{\lambda} = 0.582 \left[\frac{1+s}{1-s} \right]. \quad (5)$$

Combining Eqs. (4) and (5) yields an effective viscosity, including slip, of

$$\frac{1}{\eta_{\text{eff}}} = \frac{1}{\eta} + \frac{17.46}{n p_F d} \left[\frac{1+s}{1-s} \right]. \quad (6)$$

C. Previous experiments

The earliest experiment³ to measure slip of normal ^3He looked for corrections to hydrodynamic theory for ^3He flowing between two reservoirs through epoxy channels of various sizes and unknown roughness. The amount of slip was smaller than that predicted (for $s=0$) by approximately 30%. A later experiment⁵ measured the slip of normal ^3He enclosed in an epoxy cell similar to ours, again with surfaces of unknown roughness. The magnitude of slip was roughly 40% below the diffuse scattering prediction.

A possible explanation for the smaller slip was offered by Einzel, Panzer, and Liu,¹³ who found that the slip length can be modified by the presence of mesoscopic-scale curvature of the surfaces. The basic results will be summarized, and the possible connection to our measurements will be discussed later. In this description, the effective slip length has two contributions:

$$\frac{1}{\zeta} = \frac{1}{\zeta_0} - \frac{1}{R}. \quad (7)$$

The first term is the ordinary microscopic slip length,^{11,12} from Eq. (5). For a completely flat surface, this is the only contribution and the usual result is obtained. If the surface has any curvature of radius R , however, the second term must be included.

The theory (in its most general form and not specifically constrained to ^3He) describes mesoscopic curvature by a superposition of weak sinusoidal variations, each with wave number k and amplitude h . The results are valid only in the case that $\lambda \ll (k^{-1}, h) \ll d, \delta$ (where d is the cell dimension). Although the results are com-

plex, there are two simplifying limits. When $k\xi_0 \ll 1$, (the "stick" limit) the effective slip length is given by

$$\xi_{\text{eff}} = \xi_0 + \xi_{\omega 1}, \quad (8)$$

where ξ_0 is the ordinary, microscopic slip length and $\xi_{\omega 1}$ is a temperature-independent length given by (for a single sinusoidal variation) $\xi_{\omega 1} = -kh^2$. (We note that the stick limit is not applicable to ^3He , since $\xi_0 \approx \lambda$ and, consequently, the inequalities cannot be satisfied.) In the limit where $k\xi \gg 1$, the effective slip length is

$$\frac{1}{\xi_{\text{eff}}} = \frac{1}{\xi_0} + \frac{1}{\xi_{\omega 2}}, \quad (9)$$

where $\xi_{\omega 2}$ is again a temperature-independent term and equal to (for a single sinusoid) $1/h^2k^3$.

In both of these cases ξ_{eff} is reduced by the effects of curvature and is independent of temperature. However, since the surfaces in the earliest slip measurements were not well characterized, it is impossible to determine if this theory can resolve the discrepancy in these cases. Thus, it is desirable to measure slip with carefully controlled substrates.

Aside from the magnitude of slip, the ^3He viscosity measured in the earlier experiments was consistent with theory. Since ^4He preferentially coats the walls of a sample cell, adding small amounts of ^4He to the system may alter the ^3He boundary scattering but should not otherwise change the bulk hydrodynamic behavior. We summarize previous measurements of bulk properties of $^3\text{He}/^4\text{He}$ mixtures where the slip may have been affected by the presence of ^4He on the surfaces.

A measurement of the effective viscosity of $^3\text{He}/^4\text{He}$ mixtures was made using a quartz oscillator.⁷ The expected T^{-2} behavior was observed for a pure ^3He sample. When small amounts of ^4He were added, however, the viscosity was reduced from that of pure ^3He at low temperatures and appeared to exhibit a non- T^{-2} dependence. A later viscosity measurement⁶ using an epoxy torsional oscillator again found the expected behavior for pure ^3He . When a 4% solution of ^4He in ^3He filled the cell, however, the effective viscosity was reduced and its temperature dependence was fit quite well between about 3 and 30 mK by $\eta_{\text{eff}} \propto T^{-1.8}$. The behavior was qualitatively consistent with slip being introduced, but the temperature dependence of the dissipation when ^4He was present did not agree with predictions of slip theory for a single value of specularity. To fit the data by allowing the specularity to vary with temperature would require the specularity to approach 100% at high temperature, contrary to expectations.

Due to their geometries, neither of these measurements was sensitive to small values of slip. The presence of slip was observable only when s approached unity. We therefore designed our experiment to specifically allow precise measurements of the onset of specularity and with well-characterized surfaces.

D. Description of the experiment

The oscillator used in this experiment has a torsion element consisting of a beryllium-copper base with two dis-

tinct torsion rods, each of 1.05 mm diameter and with a 0.52 mm diameter hole through the center for the ^3He fill line. The capacitive electrodes used for drive and detection are machined from magnesium and are attached between the torsion rods to constitute the lower momenta of inertia, I_2 . The experimental region is attached above the upper torsion rod and has a moment of inertia $I_1 \ll I_2$. The oscillator is operated in the antisymmetric mode, in which the upper and lower portions oscillate out of phase. The equations describing the motion for such a double oscillator can be derived easily in analogy with the equations for a coupled pendulum. For our special case where $I_1 \ll I_2$, the resonant frequency of the antisymmetric mode is just the value it would have for the upper moment of inertia alone multiplied by the correction factor $(1 + I_1/I_2)$.¹⁴

The experimental region (I_1) consists of two silicon discs separated by a thin glass washer and epoxied together. Both silicon pieces were mechanically polished to a microscopic smoothness of approximately 20 Å. A hole through one of the discs is aligned with the fill line in the beryllium copper. Since the radius of the region between the discs is orders of magnitude larger than the cell height, d , the disc of fluid can be thought of as an infinite sheet of fluid bounded by two planes.

E. Oscillator equations

The equations of motion for a disc-shaped torsional oscillator filled with fluid are fairly standard,¹⁴ so only the results will be presented here. The results can be written in terms of a hydrodynamic parameter $x = d/\delta$. For small x , the dissipation of the fluid can be approximated by (the first correction term will be less than 1% for $x \leq 0.7$):

$$Q^{-1} = \left[\frac{2\Delta P_0}{P_0} \right] \frac{x^2}{6} = \left[\frac{2\Delta P_0}{P_0} \right] \frac{d^2 \rho \omega}{12\eta}. \quad (10)$$

Here, P_0 is the period of the empty cell and ΔP_0 is the shift in the resonant period from its value at the transition temperature to its empty-cell value, $P(T_c) - P_0$. In the expression above, Q^{-1} refers to the dissipation from the fluid alone, with the dissipation of the empty cell having been subtracted. The temperature dependence for the dissipation is contained entirely within the viscosity, η and so we expect $Q^{-1} \propto T^2$ (in the absence of slip).

If we replace the viscosity with the effective viscosity from slip theory [Eq. (6)], the dissipation becomes

$$Q^{-1} = \frac{2\Delta P_0}{P_0} \frac{d^2 \rho \omega}{12} \left[\frac{1}{\eta} + \frac{2.91}{np_F d} \left[\frac{1+s}{1-s} \right] \right]. \quad (11)$$

The term from the inverse bulk viscosity goes to zero at $T=0$ with a T^2 dependence. By choosing a small enough height, the slip term can be made non-negligible compared to the intrinsic dissipation of the oscillator, even for $s=0$. Small changes in slip, as might be caused by the addition of a thin surface film of ^4He , should then also be measurable.

After measuring the Q of the oscillator, it was driven at a constant amplitude chosen such that there were no non-

linearities evident and no self-heating. Through measurements of the drive voltage necessary to maintain the operating amplitude and the Q , the drive voltage can be converted to the dissipation as

$$Q^{-1} = (3.387 \times 10^{-6}) \times (\text{drive voltage}).$$

Data collection proceeded by monitoring the drive voltage and the resonant period of the oscillator as a function of temperature, while warming the cell.

F. Pure ^3He results

The information concerning slip and specularity is contained in the expression for the dissipation of the ^3He -filled oscillator, which should depend on temperature only through $x = d/\delta$. Slip enters through the temperature dependence of the viscous penetration depth δ . The dissipation divided by the relative period shift is a function only of x :

$$(Q^{-1})/\Delta P = \frac{2P_0}{\Delta P_0} f(x), \quad (12)$$

where $\Delta P = P(T) - P_0$ and $f(x)$ is given by¹⁴

$$f(x) = \frac{\sinh(x) - \sin(x)}{\sinh(x) + \sin(x)}. \quad (13)$$

The shape of this curve (Fig. 1) can be easily understood. At high temperatures, the fluid has a very low viscosity and is therefore not coupled to the motion of the cell. The period shift and dissipation are both small. As the temperature is lowered, the viscosity rises. More fluid is coupled to the cell motion, and the dissipation and period shift both increase. As the viscosity increases further, δ becomes comparable to the size of the cell and the fluid begins to lock to the cell motion, resulting in a lower dissipation. The period rises monotonically until nearly all the fluid is clamped to the cell motion.

The ratio given by Eq. (12) is determined by the hydrodynamic equations alone and is unaffected by slip. It is

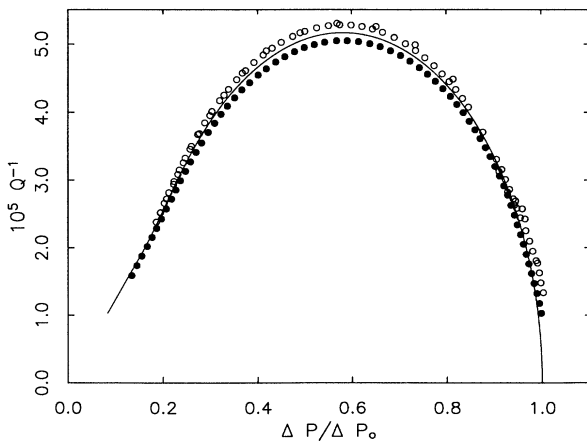


FIG. 1. Plot of dissipation as a function of fractional period shift, $\Delta P/\Delta P_0$, for the pure ^3He (●) data as well as a case with $50 \mu\text{mol}/\text{m}^2$ surface ^4He (○). The solid line is the theoretical relationship (see text).

thus instructive to examine the dissipation as a function of period shift to verify the validity of the hydrodynamic equations and the behavior of the oscillator. The experimental results are shown in Fig. 1 as solid circles. The open circles refer to data taken with ^4He on the surfaces, and will be discussed later. The solid line is the theoretical curve. The overall agreement between theory and experiment is quite good, and confirms that the oscillator is operating as expected.

Since the actual height of the cell is not accurately known from assembly, it has to be determined in the course of the experiment. The dissipation maximum occurs at $x = 2.25$ and was observed at 29.4 mK. Since the correction from slip should be small at this temperature, we use the bulk dependence, $\eta = 2.35/T^2$, which gives a viscosity at the dissipation maximum of 2.72×10^{-3} P. This yields a viscous penetration depth of $\delta = 25.8 \mu\text{m}$, corresponding to a cell height of $58.1 \mu\text{m}$.

Another determination of cell height can be made from the total period shift of the cell, which is expected to be $\Delta P = P_0(\Delta I/2I)$, where I is just the solid moment of inertia and ΔI is the fluid moment of inertia, $\pi\rho dR^4/2$. However, ΔI is not well known, since the inner radius of the glass washer, (which determines the size of the fluid region) was not measured before assembly. We sampled others from the same batch and found that their radii were $0.05 \text{ cm} \pm 10\%$. From our measurements of the various masses during assembly and the period shift obtained from Fig. 1, we estimate the cell height as $d = (46 \pm 19) \mu\text{m}$, with the uncertainty arising mainly from the radius of the fluid region.

We also made a direct measurement of the cell height. At the end of the experiment, the cell was removed from the cryostat and the spacing between the silicon plates measured using normal incidence infrared Fabry-Perot interferometry. The results were quite consistent from one trial to the next and yielded a value of $d = (57.1 \pm 2.8) \mu\text{m}$. This value has been used in the calculations throughout this paper. A fourth possible method of determining the cell height is to make a linear fit of dissipation versus T^2 and use the slope to determine d . This method is not possible in this case, as will be explained below.

The dissipation is related to the viscosity (for small $x = d/\delta$) through the relation

$$\frac{1}{Q} = \left[\frac{2\Delta P_0}{P_0} \right] \frac{d^2 \rho \omega}{12} \left[\frac{1}{\eta_{\text{eff}}} \right]. \quad (14)$$

With $d = 57.1 \mu\text{m}$, $2\Delta P_0/P_0 = 1.244 \times 10^{-4}$, and including slip through Eq. (6), Eq. (14) reduces to

$$\frac{1}{Q} = 2.76 \times 10^{-7} \left[\frac{1}{\eta_{\text{bulk}}} + 2.26 \left[\frac{1+s}{1-s} \right] \right]. \quad (15)$$

The data for dissipation is plotted against T^2 in Fig. 2 for the pure ^3He sample. For reference, the line produced from slip theory for completely diffuse scattering [by inserting $\eta_{\text{bulk}} = 2.35/T^2$ and $s = 0$ into Eq. (15)] is also shown. The data taken with ^4He present will be discussed later. The most striking feature in this figure is

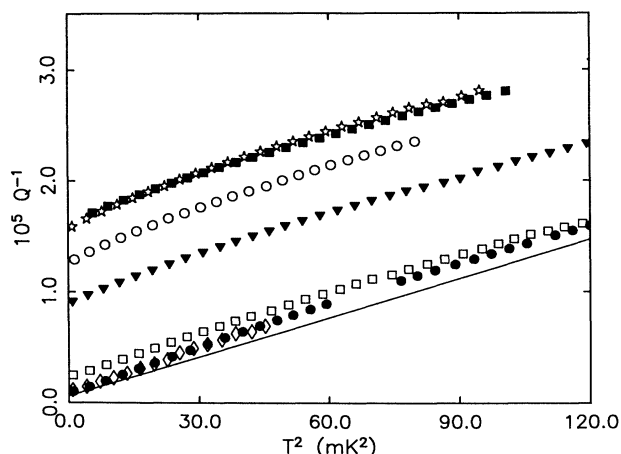


FIG. 2. The dissipation (Q^{-1}) is plotted vs the square of the temperature as solid circles for the pure ^3He sample. The solid line is the theoretical expectation for completely diffuse scattering, as described in the text. For the data taken with surface ^4He , the symbols refer to the pure ^3He = \bullet ; $20.6 \mu\text{mol}/\text{m}^2$ = \diamond ; $30.0 \mu\text{mol}/\text{m}^2$ = \square ; $39.2 \mu\text{mol}/\text{m}^2$ = \blacktriangledown ; $57.7 \mu\text{mol}/\text{m}^2$ = \circ ; $86.6 \mu\text{mol}/\text{m}^2$ = \star ; $115.4 \mu\text{mol}/\text{m}^2$ = \blacksquare .

that the dissipation is *not* linear in T^2 . This means that the slope cannot be used to determine the cell height, and a determination of the magnitude of slip and/or specularly becomes impossible.

The most obvious explanation for the non- T^2 dependence would be some sort of experimental artifact. However, the agreement between data and theory in Fig. 1 verifies that the cell is behaving as expected. The χ factor, which quantifies the amount of superfluid that is coupled to the cell motion, was also measured by filling the cell with ^4He . It was found to be less than 1%, which confirms that there are no unusual geometric effects.

Another possible source of error involves the thermometry. However, the data was taken, while warming in constant field at a rate slow enough to ensure thermal equilibrium between the cell and the thermometer. Various constant offsets in temperature (up to ± 0.2 mK) were also arbitrarily introduced, but none caused the dissipation to revert to the expected behavior. The dissipation was also substantially larger than the background at all temperatures.

Since many of the previous viscosity^{6,15,16} measurements for solutions of $^3\text{He}/^4\text{He}$ report T^n power laws (with $n > -2$), we attempted to fit the ^3He data in Fig. 2 to the form $Q^{-1} = -AT^n + B$. A good fit can be obtained over the temperature range shown for $n = 1.7(\pm 0.05)$. This power-law behavior will be further discussed once the effects from adding the ^4He are described.

G. Effects of surface ^4He

Once all the pure ^3He data had been taken, the cell was warmed to a few Kelvin, while being pumped on. After the ^3He was removed, the temperature was raised to around 8–10 K, ^4He was added to the cell and allowed to anneal at 6–10 K for several hours in order to uniformly coat the surfaces. The temperature was then reduced to

below 1 K and the ^3He was readmitted slowly. Coverages of ^4He equivalent to 20.8, 30, 39.2, 57.7, 86.6, and $115.4 \mu\text{mol}/\text{m}^2$ were added to the cell. Finally, $230 \mu\text{mol}/\text{m}^2$ was attempted, but the data was unusable, since the heat leak into the cell was too large at this coverage. The surface area enclosed by the experimental region was predominantly that of the heat exchanger to cool the ^3He and was measured using the standard Brunauer-Emmett-Teller¹⁷ method to be 26.0 m^2 . With this large area, even a submonolayer coverage of ^4He corresponded to an easily measurable volume of gas at room temperature.

Although there is a small increase in the overall dissipation for the data with surface ^4He , comparison of the data for dissipation versus period shift (Fig. 1) with theory shows reasonable agreement. The data shown in this figure (\circ) is for the $50 \mu\text{mol}/\text{m}^2$ coverage, and is very similar for other coverages. The overall increase in dissipation with the addition of ^4He has also been observed in another torsional oscillator experiment.¹⁶ This plot shows that it is primarily the temperature dependence of the dissipation and period that are affected by the addition of the ^4He , rather than their ratio.

If Q^{-1} is plotted against T^2 , a constant nonzero specularly is expected to increase only the zero-temperature intercept. The data sets for dissipation plotted against T^2 are shown for these ^4He coverages, along with the pure ^3He data in Fig. 2. The shape of the curves when ^4He is present are roughly similar to that of the ^3He curve with only the value of the $T=0$ intercept changing. Aside from the temperature dependence of the bulk term, the data demonstrates qualitative agreement with slip theory, in which increasing specularly increases only the dissipation intercept. Thus it appears that surface ^4He films do induce specular scattering in a manner qualitatively consistent with slip theory. However, some other factor seems to be affecting the temperature-dependent or bulk viscosity term.

If we fit these various curves to a power law ($AT^n + B$), as was done for the ^3He , the best fits occur for values of n between 1.65 and 1.75. Forcing all to the same exponent of $n = 1.70$ (with slope and intercept as adjustable parameters) produces the fits shown in Fig. 3. The ^4He coverages of 20.6 and $115.4 \mu\text{mol}/\text{m}^2$ are not shown, since the data overlap that of the pure ^3He and the $86.6 \mu\text{mol}/\text{m}^2$, respectively.

At least one previous experiment⁶ found that the power law for the temperature dependence of the bulk viscosity dropped when ^4He was added to the system. The major differences between that experiment and ours are the size and surfaces of the cell. The effects from the finite size of the cell are well known, and the cell is actually similar in size to the one used in Ref. 4. Attributing the unusual behavior to some yet unknown effect arising from finite-size corrections can be ruled out. However, unlike the earlier experiments, we polished our surfaces to a mirror-smooth finish. Any effect caused by the smoothness of the surfaces might also be observed on rougher surfaces, which had been smoothed by the addition of ^4He . It therefore seems plausible that the microscopic surface geometry may affect the bulk viscosity behavior.

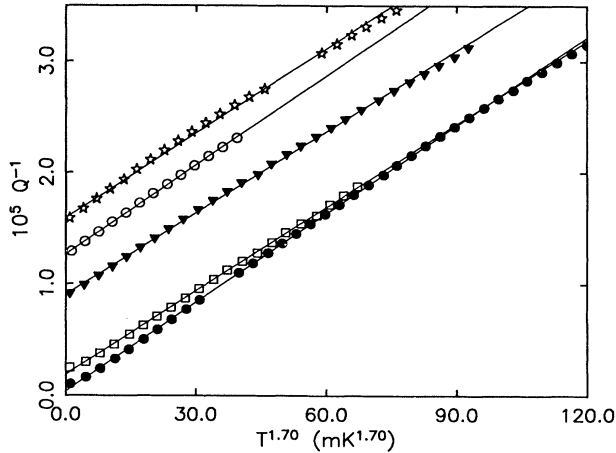


FIG. 3. The ${}^3\text{He}$ dissipation plotted against $T^{1.70}$ for the pure ${}^3\text{He}$ and some of the cases with surface ${}^4\text{He}$. The symbols are the same as in Fig. 2 and the solid lines are linear fits to the data.

Throughout this discussion, we have assumed that the limiting temperature dependence of the viscosity is T^{-2} . Most experiments performed with torsional oscillators and geometries similar to this experiment have measured viscosities that closely follow the expected Fermi-liquid dependence. Finite-size effects⁵ can lead to an effective viscosity that increases rather more slowly than T^{-2} . Some previous experiments^{19,20} with larger geometries fabricated without special care as to surface polish have also observed a temperature dependence of the viscosity different from the expected T^{-2} behavior. Carless *et al.*¹⁹ found that the viscosity deviated from the expected T^{-2} form below 5 mK by 20% of the expected low-temperature value. By contrast, Krusius *et al.*²⁰ found a larger departure below 4 mK. Neither of these results have been explained. In our experiment the viscosity displays a non- T^{-2} behavior over a wider temperature range and is qualitatively different from the earlier results. It is therefore important to bear in mind that several experiments fail to obtain the Fermi-liquid form for the viscosity. It is possible that surface finishes have a determining role in these measurements and that the effect of the boundary condition on the measured viscosity is larger than implied by theory.

H. Analysis of the data

It is instructive to examine the temperature dependence of the parameter x when slip is included. The square of x follows from the relations for viscous penetration depth and effective viscosity:

$$\begin{aligned} x^2 &= \frac{d^2}{\delta^2} = \frac{d^2 \rho \omega}{2} \left[\frac{1}{\eta} + \frac{2.91}{np_F d} \left(\frac{1+s}{1-s} \right) \right] \\ &= 0.0133 \left[\frac{T^2}{2.35} + 2.26 \left(\frac{1+s}{1-s} \right) \right]. \end{aligned} \quad (16)$$

The values for $x(T)$ obtained from the dissipation data are plotted against the temperature in Fig. 4. As expect-

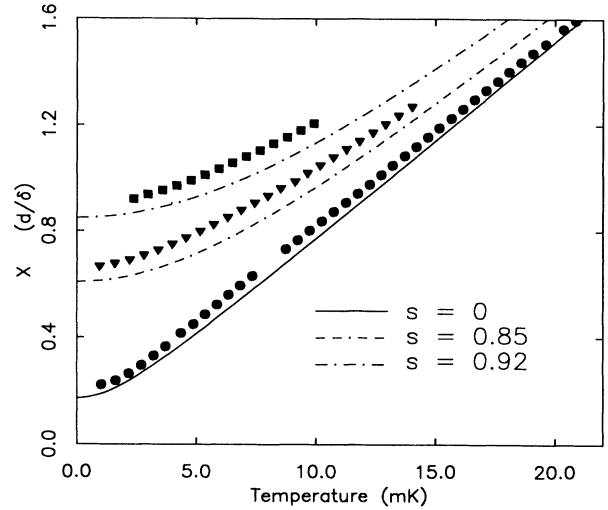


FIG. 4. The hydrodynamic parameter $x(d/\delta)$ is plotted as a function of temperature for the pure ${}^3\text{He}$ and some of the runs with surface ${}^4\text{He}$ present. The symbols correspond to the same ${}^4\text{He}$ coverages as in previous figures and the lines correspond to theory for the specularity values shown.

ed, the plots of $x(T)$ for the data sets in which surface ${}^4\text{He}$ is present show substantial curvature due to the slip term. The data for the pure ${}^3\text{He}$, however, is approximately linear between 3 and 20 mK but with a substantial $T=0$ intercept. This suggests the possibility of a temperature-independent length, which dominates the bulk behavior of the system at low temperatures where the viscous penetration depth diverges, together with a very small slip term.

Since a single temperature-independent value for s cannot adequately describe the data, it seems worthwhile to examine what happens if we use s as a temperature-dependent fitting parameter. The results are shown in Fig. 5. The specularity needed to force agreement between slip theory and the data decreases as temperature is lowered for all the data sets. All the length scales in

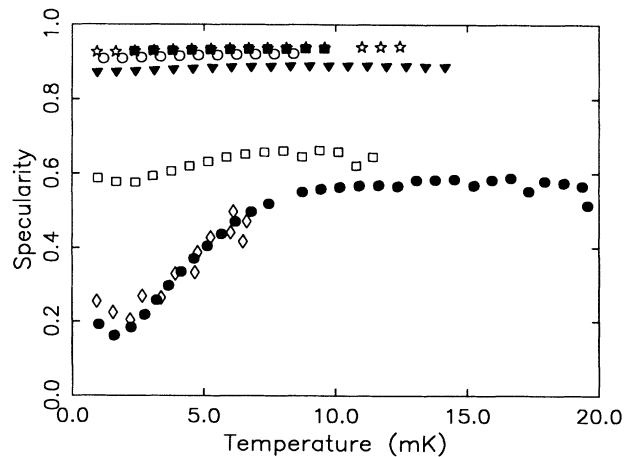


FIG. 5. The values for specularity required to make the data conform to slip theory are shown for the various data sets. The symbols correspond to those of Fig. 2.

^3He (mean free path, viscous penetration depth, mean thermal wavelength) increase as temperature is lowered. Therefore, any atomic roughness on the surface will be getting smaller relative to these length scales, implying that specularly should increase as the temperature is reduced. We therefore do not believe that the anomalous temperature dependence should be ascribed to the specularly.

All the previous equations from slip theory have implicitly assumed macroscopically and mesoscopically flat surfaces. A model for slip from surfaces having large mesoscopic curvature has been proposed,¹³ which can modify the microscopic slip length. The surface smoothness of our silicon was characterized with an Alpha-Step profiler. Figure 6 reveals curvature on various length scales. Scans were taken at many different areas on the silicon, and these present typical results. For a horizontal length scale of k^{-1} (in analogy with the theory that characterizes the curvature as a superposition of sinusoidal wave functions) of about $50\ \mu\text{m}$, the characteristic features had heights (h) of around $20\ \text{\AA}$. For $k^{-1} \sim 100\ \mu\text{m}$, $h \sim 100\ \text{\AA}$. Finally, for $k^{-1} \sim 3000\ \mu\text{m}$, $H \sim 600\ \text{\AA}$.

The mesoscopic curvature theory is valid only in the limit that $\lambda \ll (k^{-1}, h) \ll d, \delta$. For this experiment (T in mK), $\lambda \sim 86/T^2\ \mu\text{m}$, $\delta \sim 755/T\ \mu\text{m}$ (for no slip), and $d \sim 57\ \mu\text{m}$. Clearly, over the temperature range of interest, these limitations cannot be met. Therefore, we can only estimate the size of the modifications to the microscopic slip length due to the measured mesoscopic curvature, which we find to be extremely small. Even curvature amplitudes as large as $h = 1$ (for $k^{-1} = 20\ \mu\text{m}$) produce only a slight decrease of s , and only at the lowest temperatures. Therefore, it seems unlikely that the deviation of the data from theoretical expectations can be attributed to mesoscopic curvature.

Although the unexpected bulk behavior of the data precludes any quantitative assessment of the slip or specularly, it is clear that specularly is being introduced

by the surface ^4He . The manner in which the dissipation intercept change can still yield information about the mechanism for the introduction of specularly. Specifically, it is noteworthy that there was no discernible change in dissipation for the lowest coverage of ^4He , $20.8\ \mu\text{mol}/\text{m}^2$ (which should be just over one monolayer⁸). This behavior is illustrated more clearly in Fig. 7. Although the values of s shown do not necessarily quantify the specularly correctly, the overall behavior of the specularly is meaningful. The ^4He coverage is given in approximate monolayer equivalents, using $32\ \mu\text{mol}/\text{m}^2$ for the first two layers and $13\ \mu\text{mol}/\text{m}^2$ for subsequent layers.⁸ It is clear that specularly turns on rather suddenly for ^4He coverages greater than about 2 monolayers. The rapid increase in specularly covers only 1–2 monolayers, but the specularly continues to rise slowly for additional amounts of ^4He up to about 8 monolayers. The data taken at roughly 16 monolayers, which had a large uncertainty, had a specularly slightly below that of the 8 monolayer data.

From the results in Fig. 7, we conclude that the specularly induced by surface ^4He is not a result of the geometric smoothing of atomic-sized corrugations on the surfaces, since there is no effect at the lowest coverage. In addition, it seems unlikely that substantial smoothing on the atomic length scale would continue to occur for coverages above a few monolayers. Second, any effects caused by the localized magnetic layer of ^3He next to the surface can be ruled out. For the $20.8\ \mu\text{mol}/\text{m}^2$ coverage of ^4He , the entire first layer of ^3He has been replaced with nonmagnetic ^4He , so any effects caused by the magnetic state of this layer should be evident at even this lowest coverage.

The relatively rapid onset of specularly at 2 monolayers of ^4He coincides with the thickness at which a Kosterlitz-Thouless transition was measured by Freeman¹⁸ for ^4He films covered by bulk ^3He (it was impossible to observe this transition directly in our experiment).

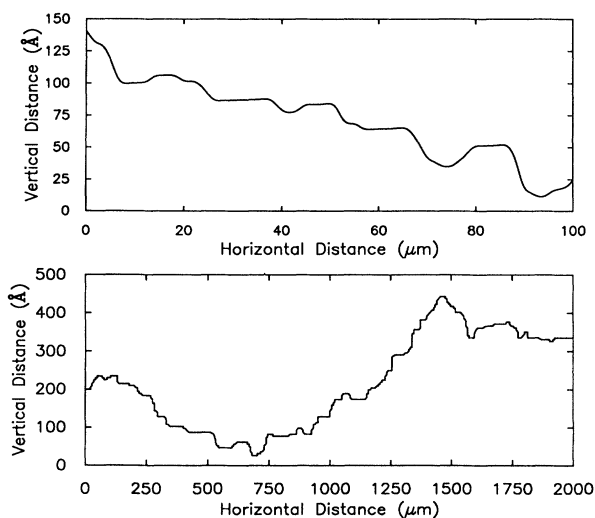


FIG. 6. Surface scans of the silicon plates produced by the Alpha-Step profiler for two different horizontal length scales.

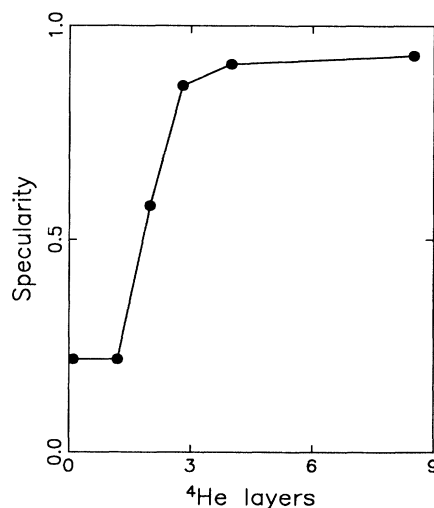


FIG. 7. The specularly, taken from Fig. 5 at 3 mK, is plotted as a function of the surface ^4He coverage. The solid line is a guide to the eye.

This suggests that the superfluidity of the ^4He film might be responsible for the specular scattering of the ^3He . However, since the specularly does not immediately jump to 100% at this ^4He thickness, there must continue to be some coupling between the ^3He and the substrate. It is not clear how momentum is transferred between the ^3He fluid and the solid surface across the surface superfluid layer of ^4He . It is possible that some fraction of the ^3He atoms propagate ballistically through the ^4He film to exchange momentum with the substrate. This fraction would decrease as the ^4He film thickness increased. At large thicknesses, the finite solubility of ^3He into the ^4He may cause the effect to saturate. It has also been proposed²¹ that momentum transfer occurs via vortex lines threading the ^4He film. Thicker films would support fewer vortices and decrease the total momentum transfer.

Also consistent with the data is the model proposed by Hall,⁴ which describes the momentum decoupling as a consequence of the physical separation of the ^3He from the substrate due to the intervening ^4He film. If the attractive forces between ^4He and ^3He are much smaller than those between the substrate and the ^3He , scattering of ^3He from a ^4He surface might be specular, while scattering of ^3He from the substrate might be diffuse. For thin enough ^4He films, the ^3He would still experience some of the substrate potential and scatter somewhat diffusely. As the ^4He film thickness increased, however, the ^3He would be kept further from the substrate and be able to exchange less momentum with the substrate. The dependence of specularly on ^4He film thickness would depend primarily on the spatial extent of the van der Waals potential from the substrate. The finite solubility of ^3He into ^4He for the thicker films may cause this effect to saturate. It is not known how much ^3He dissolves into thin films of ^4He covered by bulk ^3He . However, a third sound experiment²² performed on thin films of $^3\text{He}/^4\text{He}$ solutions obtained data consistent with complete phase separation for ^4He film thicknesses up to about 6 monolayers and varying amounts of ^3He . A simple extension of a theory of Lahuerte *et al.*²³ from the case of mixture films to films of ^4He covered by ^3He also predicts nearly complete phase separation for ^4He films a few layers thick. From these results alone, it is not clear which (if either) of these explanations is correct. One might be able to discriminate between these explanations by measuring the slip or specularly for both a superfluid ^4He film and a solid ^4He film in the same system.

III. SUPERFLUID ^3He EXPERIMENT

A. Boundary conditions for superfluid ^3He

The theory²⁴⁻²⁶ that describes the effects of specular scattering at a boundary finds a slight enhancement in the transverse components of the order parameter near a specularly reflecting surface. For completely diffuse scattering, the transverse components of the order parameter drop from their bulk value to zero within about one coherence length from the surface. Since the superfluid density of ^3He is proportional to the square of

the order parameter, the superfluid fraction of ^3He would be suppressed near diffusely scattering boundaries.

The zero-temperature coherence length of ^3He is given by

$$\xi_0 = \frac{\hbar v_F}{2\pi k_B T_c} \quad (17)$$

and ranges from about 720 Å at 0 bar to 160 Å at 29 bar. For ^3He enclosed in structures smaller than a few thousand angstroms, a substantial fraction of the fluid will be within one coherence length of a boundary, leading to suppression of the superfluid fraction and the transition temperature (providing the surfaces scatter diffusely). Specular scattering should cause no such suppression. For a porous medium with diffusively scattering surfaces, the amount of suppression depends on the ratio of average pore size to the coherence length. The coherence length can be varied, since it is strongly dependent on pressure.

Since the geometry is not uniform or well characterized in the pores, the expected depression of T_c can only be estimated. We approximate the porous geometry of a packed powder by a series of cylinders of radius R . In such an idealized geometry, the superfluid transition temperature is given by²⁵

$$T_c = T_c^0 e^{-3.47\xi_0^2/R^2} \quad (18)$$

where T_c^0 is the bulk transition temperature and ξ_0 is the zero-temperature coherence length (at a given pressure).

B. Previous experiments

Following the prediction of superfluid suppression by diffusively scattering surfaces, several experiments observed the effect. The first experiment²⁷ observed a reduced transition temperature for superfluid flow through micrometer-sized channel in a porous membrane. A subsequent fourth sound experiment²⁸ performed on ^3He confined in packed powder geometries found that both the transition temperature and superfluid density were reduced from bulk. The amount of suppression increased as the pore size decreased. Later experiments^{29,30} used a variety of materials to confine the ^3He and found reasonably good agreement with the theory assuming diffuse scattering at the walls. This is consistent with observations in the normal fluid, which suggested that ^3He scattering from solid surfaces might *always* be diffuse unless the surfaces have been coated with ^4He .

An experiment by Freeman *et al.*⁸ found similar superfluid suppression for ^3He confined between thinly-spaced mylar sheets. However, they also observed that the addition of a few monolayers of ^4He to the surfaces reduced the amount of suppression, as would be expected for increased specular scattering of the ^3He . A later experiment³¹ obtained similar results using fourth sound measurements of ^3He in packed powders. They found no reduction in the superfluid suppression by adding a single monolayer of ^4He to the surfaces, but a substantial reduction for a 3 monolayer ^4He coverage. In contrast, experiments of film flow of superfluid ^3He (Ref. 32) demonstrat-

ed a crossover from diffuse to specular scattering with the addition of a single monolayer of ^4He . Measurements of the superfluid density and transition temperature for ^3He in a confined geometry are, therefore, useful indicators of the surface scattering.

C. Description of the experiment

A torsional oscillator¹⁴ was used as the measuring device for the superfluid ^3He . The quantity of interest here was the shift in resonant period, from which the superfluid fraction could be deduced. A beryllium copper body with a single torsion rod was attached to a cylindrical epoxy container that housed the experimental region and constituted the head of the oscillator. The substrate was made from silver powder with a nominal diameter of 700 Å, packed to 68% of solid density. Experimental details may be found elsewhere.^{2,14,33}

Experiments were first carried out on the pure ^3He sample, and, once they were complete the addition of the ^4He to the surfaces proceeded in the same manner as the normal ^3He experiment described earlier. We added approximately $50 \mu\text{mol}/\text{m}^2$ of ^4He to the surfaces, or about 3.5 monolayers. At this ^4He coverage, the data from the normal fluid experiment indicated nearly complete specularly. After taking the data for this ^4He coverage, an additional $15 \mu\text{mol}/\text{m}^2$ was added to bring the total ^4He coverage to about 4.5 monolayers.

D. Results for pure ^3He

The transition temperatures measured for various pressures are shown in Table I, including the T_c for bulk at each pressure. The data in the last column will be discussed later. In most cases, the bulk transition was manifested as a kink in the temperature trace from the lanthanum-doped cerium magnesium nitrate thermometer. These temperatures agreed very well (within $50 \mu\text{K}$) with the expected T_c for bulk. When a kink was not clearly visible, the expected bulk T_c is noted.

The theory describing the depression of transition temperature in a confined geometry of long cylindrical pores (with diffusely scattering boundaries) is not applicable to this geometry. However, if one simply uses Eq. (18) as an estimate with $R = 1000 \text{ Å}$ and the coherence length given by Eq. (17), the “expected” values for the depressed T_c agree remarkably well (within $50 \mu\text{K}$) with those obtained experimentally for all but 0 bar.

TABLE I. Transition temperatures for the confined ^3He with 3.5 monolayers of surface ^4He present. The values for pure ^3He and bulk are repeated here for comparison. The data at 0 bar was noisy, so a determination of the transition temperature was not possible.

| Pressure | T_c (pure ^3He) | T_c (bulk) | T_c (with surface ^4He) |
|----------|-----------------------------|--------------|-------------------------------------|
| 0 bar | 0.87 mK | 0.93 mK | |
| 5 bar | 1.28 mK | 1.48 mK | 1.44 mK |
| 17 bar | 1.97 mK | 2.14 mK | 2.12 mK |
| 24 bar | 2.22 mK | 2.32 mK | 2.28 mK |
| 28 bar | 2.29 mK | 2.40 mK | 2.29 mK |

Once T_c and $P(T_c)$ were determined for a given pressure, the period versus temperature data was converted to superfluid density (ρ_s/ρ) as a function of T/T_c (Ref. 33). The results for the various pressures are shown in Fig. 8. Qualitatively, the behavior conforms quite well with expectations. The coherence length decreases with increasing pressure leading to an increase of the superfluid fraction.

E. Effect of surface ^4He

After adding ≈ 3.5 monolayers of ^4He , for pressures below 17 bar the transition temperatures were no longer depressed below bulk as they had been for the pure ^3He . In addition, the superfluid density was enhanced at these pressures. There may be two separate effects suppressing the superfluidity—the diffuse scattering from the surfaces and the bending terms required in the order parameter.³⁴

The transition temperatures observed with 3.5 monolayers of ^4He on the surfaces are shown in Table I. At the lower pressures, T_c is nearly restored to its bulk value. Above 17 bar, this restoration of transition temperature began to decrease (the effect being quite small, since T_c is suppressed only slightly at these pressures). At 28 bar, the enhancement had completely disappeared. The pressure could not be raised above about 29 bar because of solidification of the ^3He in the fill line. The behavior of the superfluid fraction paralleled that of the transition temperature. These results together with the discussion of the solidification of the surface helium are presented more completely in Ref. 2.

The results of the normal ^3He experiment suggest that a ^4He coverage of this thickness should scatter ^3He with a very high degree of specularity. The nearly complete restoration of transition temperature tends to confirm this assumption, even though ρ_s/ρ is not restored to its bulk value. If there were no solidification of the ^4He film, the superfluid fraction would presumably continue to in-

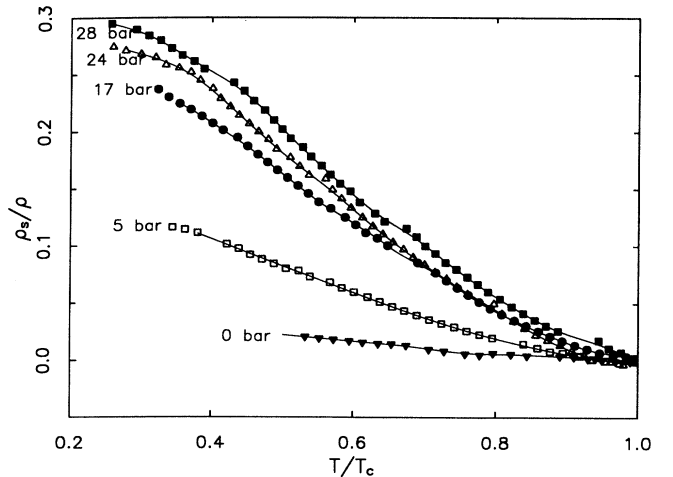


FIG. 8. The superfluid fraction is shown for various pressures as a function of T/T_c , with T_c taken as the measured transition temperature, not that of bulk. The solid lines are guides to the eye.

crease with pressure. Solidification of the surface ^4He film completely destroys its specular scattering properties for ^3He , reverting to the full amount of suppression observed for the uncoated surfaces (diffuse scattering). Thus, any other possible mechanism for reducing the superfluid fraction with increasing pressure (above 17 bar) seems unlikely.

After taking data at this coverage of ^4He , a coverage of $65 \mu\text{mol}/\text{m}^2$ (or roughly 4.5 monolayers) was examined. At low pressures, the superfluid fraction data and T_c closely matched that from the lower ^4He coverage. This confirms our supposition that the specularly was nearly complete for the lower coverage and that the remaining suppression is due to some other factor. At higher pressures, the superfluid fraction continued to be enhanced relative to the pure ^3He result to much higher pressures than for the thinner ^4He coverage. We found that solidification commences at approximately 17 bar for the thinner film and at about 25 bar for the thicker film.

This observation provides clues about the mechanism for induction of specularly by ^4He . Since the specularly is destroyed when the ^4He film is solidified, the superfluidity of the ^4He must be responsible for specular scattering. For films too thin or pressures too high for the ^4He to be fluid, the scattering remains diffuse just as for no ^4He coverage at all.

IV. SUMMARY AND CONCLUSIONS

The combination of results from the two experiments provides a much better understanding of the ^3He scattering processes that occur at a solid surface. However, many questions were raised by the data and many others remain unanswered.

One of the first questions addressed was whether or not ^3He could be made to scatter specularly from a solid substrate by highly polishing the surfaces and thus identify the relevant ^3He scattering length, k_F^{-1} or Λ . Although the oscillator appeared to be operating as expected, the data did not conform to theory. Consequently, it was impossible to unambiguously determine the slip and this question remains unanswered. However, the data suggests that the local smoothness might affect the bulk viscosity measurement in a manner other than that predicted by slip theory. If feasible, it would be very instructive to roughen the surfaces of this cell and observe whether or not the temperature dependence of the effective viscosity reverts to the $1/T^2$ dependence.

In spite of the unexpected behavior of the bulk viscosity, the effect of adding ^4He was unmistakable. While there was no effect for thinner layers of ^4He , the specularly of the surface increased dramatically with the addition of 2 or more monolayers of ^4He . The specularly continued to increase as additional ^4He was deposited until about 8 monolayers were completed. The fact that specularly was induced rather suddenly at the same ^4He coverage as is necessary to cause superfluidity of the ^4He suggested that the two effects are related. The mechanism for coupling momentum between the surfaces and the ^3He across an intervening superfluid layer is not known, nor is it understood why the specularly has a thickness dependence between about 2 and 8 monolayers, though this might possibly result from the finite solubility of ^3He into ^4He .

There are two hypotheses concerning the mechanism for inducing specularly that are consistent with the data. The first assumes that the superfluidity of the ^4He film is responsible for the specularly. Most of the incident ^3He atoms are reflected specularly by the $^3\text{He}/^4\text{He}$ interface; those which penetrate the ^4He may still exchange some of their momentum with the substrate. The second hypothesis assumes that the ^4He acts as a spacer to keep the ^3He away from the attractive potential of the substrate. Less momentum is exchanged as the ^4He film thickness is increased. The phase of the ^4He is not important to the latter hypothesis, while it is crucial to the former. The hypothesis that the superfluidity of the ^4He film is responsible for the specular scattering was investigated in the superfluid ^3He experiment by pressurizing the ^3He to solidify the ^4He film. The effects of specular scattering caused by the addition of the ^4He were entirely removed when the ^4He solidified, affirming that the former hypothesis is correct.

ACKNOWLEDGMENTS

We are indebted to K. R. Lane for help in operating the cryostat. The authors have benefited from a number of interesting discussions with Dr. D. Einzel, Dr. M. Freeman, Dr. E. Thuneberg, Dr. E. N. Smith, Professor V. Ambegaokar, Professor V. Elser, Professor J. D. Reppy, Professor D. M. Lee, and Professor R. C. Richardson. This research was supported by the National Science Foundation (NSF) through DMR 88-20170, DMR 91-23857 and the Cornell Materials Science Center through DMR 88-18588.

*Present address: Intel, Hillsboro, Oregon 97124.

¹S. M. Tholen and J. M. Parpia, *Phys. Rev. Lett.* **67**, 334 (1991).

²S. M. Tholen and J. M. Parpia, *Phys. Rev. Lett.* **68**, 2810 (1992).

³J. P. Eisenstein, G. W. Swift, and R. E. Packard, *Phys. Rev. Lett.* **45**, 1199 (1980).

⁴H. E. Hall, in *Proceedings of the European Physical Society*, Haifa, Israel, 1974, edited by C. G. Kuper, S. G. Lipson, and M. Revzen (Wiley, New York, 1974).

⁵J. M. Parpia and T. L. Rhodes, *Phys. Rev. Lett.* **51**, 805 (1983).

⁶D. A. Ritchie, J. Saunders, and D. F. Brewer, *Phys. Rev. Lett.* **59**, 465 (1987).

⁷D. S. Betts, D. F. Brewer, and R. Lucking, in *Proceedings of the 13th International Conference on Low Temperature Physics*, Boulder, Colorado, 1972, edited by K. D. Timmerhaus, W. J. O'Sullivan, and E. F. Hammel (Plenum, New York, 1976).

⁸M. R. Freeman *et al.*, *Phys. Rev. Lett.* **60**, 596 (1988); M. R. Freeman and R. C. Richardson, *Phys. Rev. B* **41**, 1101

- (1990).
- ⁹G. Baym and C. Pethick, in *The Physics of Liquid and Solid Helium*, edited by K. H. Bennemann and J. B. Ketterson (Wiley, New York, 1978).
- ¹⁰It should be noted that some of these viscosity coefficients were measured using a thermometer calibrated against the melting curve of ^3He measured by Halperin *et al.* [J. Low Temp. Phys. **31**, 617 (1978)]. If we convert to the melting curve as measured by Greywall [Phys. Rev. B **33**, 7520 (1986)], as is used in this experiment, the value for the proportionality constant in the viscosity is lowered by approximately 10%. The value of $2.35 \text{ mK}^2 \text{ P}$ has taken this correction into account.
- ¹¹H. H. Jensen *et al.*, J. Low Temp. Phys. **41**, 473 (1980).
- ¹²D. Einzel *et al.*, J. Low Temp. Phys. **53**, 695 (1983).
- ¹³D. Einzel, P. Panzer, and M. Liu, Phys. Rev. Lett. **64**, 2269 (1990), Physica B **165&166**, 555 (1990).
- ¹⁴S. M. Tholen, Ph.D. thesis, Cornell University, 1992.
- ¹⁵M. J. Lea, P. W. Retz, and P. Fozooni, Phys. Lett. A **117**, 477 (1986).
- ¹⁶M. P. Bertinat *et al.*, Phys. Rev. Lett. **28**, 472 (1972).
- ¹⁷S. Brunauer, P. H. Emmett, and E. Teller, J. Am. Chem. Soc. **60**, 309 (1938).
- ¹⁸M. R. Freeman, Ph.D. thesis, Cornell University, 1988.
- ¹⁹D. C. Carless *et al.*, J. Low Temp. Phys. **50**, 583 (1983).
- ²⁰M. Krusius *et al.*, Fiz. Nizk. Temp. **12**, 339 (1986) [Sov. J. Low Temp. Phys. **12**, 191 (1986)].
- ²¹C. Wang and L. Yu, Physica B **169**, 529 (1991).
- ²²F. M. Ellis *et al.*, Phys. Rev. Lett. **46**, 1461 (1981).
- ²³J. P. Lahuerte *et al.*, J. Phys. (Paris) **47**, 39 (1986).
- ²⁴V. Ambegaokar, P. de Gennes, and D. Rainer, Phys. Rev. A **9**, 2676 (1974).
- ²⁵L. H. Kjøldman, J. Kurkijärvi, and D. Rainer, J. Low Temp. Phys. **33**, 577 (1978).
- ²⁶W. Zhang, J. Kurkijärvi, and E. V. Thuneberg, Phys. Lett. **109A**, 238 (1985).
- ²⁷M. T. Manninen and J. P. Pekola, J. Low Temp. Phys. **52**, 497 (1983).
- ²⁸T. Chainer, Y. Morii, and H. Kojima, J. Low Temp. Phys. **55**, 353 (1984).
- ²⁹V. Kotsubo *et al.*, Jpn. J. Appl. Phys. **26**, 143 (1987).
- ³⁰V. Kotsubo, K. D. Hahn, and J. M. Parpia, Phys. Rev. Lett. **58**, 804 (1987).
- ³¹D. Kim *et al.*, Physica B **165&166B**, 637 (1990); see also K. S. Ichikawa *et al.*, Phys. Rev. Lett. **58**, 1949 (1987).
- ³²S. C. Steel *et al.*, Physica B **165&166B**, 599 (1990).
- ³³T. Hall *et al.*, J. Low Temp. Phys. (to be published).
- ³⁴E. V. Thuneberg (private communication).